Effect of Variable Amplitude Blocks' Ordering on the Functional Fatigue of Superelastic NiTi Wires
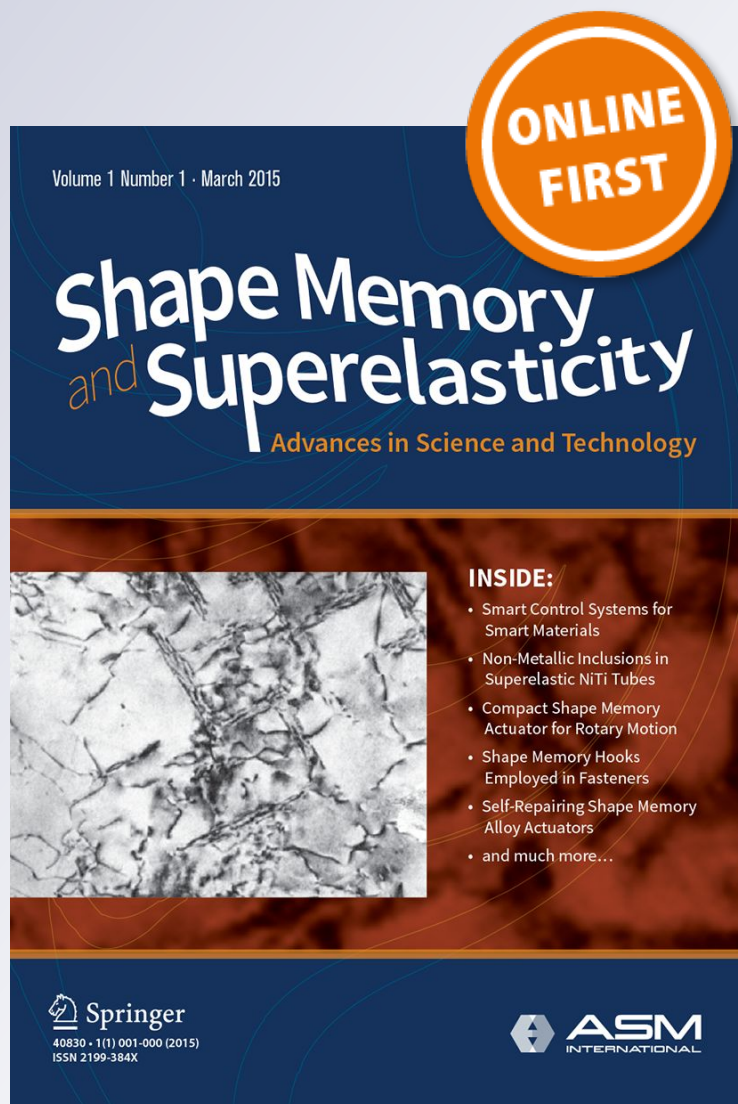
Hugo Soul & Alejandro Yawny

Springer

CrossMark

TECHNICAL ARTICLE

Effect of Variable Amplitude Blocks' Ordering on the Functional Fatigue of Superelastic NiTi Wires

Hugo Soul[1] · Alejandro Yawny[2]

Abstract Accumulation of superelastic cycles in NiTi uniaxial element generates changes on the stress–strain response. Basically, there is an uneven drop of martensitic transformation stress plateaus and an increase of residual strain. This evolution associated with deterioration of superelastic characteristics is referred to as "functional fatigue" and occurs due to irreversible microstructural changes taking place each time a material domain transforms. Unlike complete cycles, for which straining is continued up to elastic loading of martensite, partial cycles result in a differentiated evolution of those material portions affected by the transformation. It is then expected that the global stress–strain response would reflect the previous cycling history of the specimen. In the present work, the consequences of cycling of NiTi wires using blocks of different strain amplitudes interspersed in different sequences are analyzed. The effect of successive increasing, successive decreasing, and interleaved strain amplitudes on the evolution of the superelastic response is characterized. The feasibility of postulating a functional fatigue criterion similar to the Miner's cumulative damage law used in structural fatigue analysis is discussed. The relation of the observed stress–strain response with the transformational history of the specimen can be rationalized by considering that the stress-induced transformation proceeds via localized propagating fronts.

Keywords Functional fatigue · Superelasticity · Variable amplitude

✉ Hugo Soul
hugo.soul@cab.cnea.gov.ar

Alejandro Yawny
yawny@cab.cnea.gov.ar

1 CONICET, Physics of Metals, Centro Atómico Bariloche, S.C. de Bariloche, Río Negro, Argentina

2 CNEA/CONICET, Physics of Metals, Centro Atómico Bariloche, S.C. de Bariloche, Río Negro, Argentina

Introduction

Due the number of commercially successful applications, near-equiatomic NiTi alloys constitute the most relevant family among the so-called shape memory alloys. The exhibited superelastic behavior allows for NiTi members to develop high recoverable strains (up to 8–10%) [1]. The occurrence of the stress-induced martensitic transformation before generalized plastic yielding provides for extraordinary flexibility and kink resistance of slender elements [2]. The good corrosion resistance and superior biocompatibility attributed to NiTi alloys have boosted them for their use in orthodontics, endoscopic catheters, and different types of stents [3–6]. Other applications concern the damping capabilities associated with the hysteretic characteristics of the strain–stress curve in a superelastic cycle [7, 8]. The mechanical response of NiTi elements to temperature loading is used for actuators in control systems [9, 10], mechanical releasing devices [11, 12], and tube seals [13]. On the other hand, by imposing a stress-induced transformation, the latent heat absorbed during reverse transformation is exploited as the functioning principle of refrigerator systems [14, 15].

A common aspect concerning many of the applications is that NiTi elements are subjected to repetitive loading

🌀 Springer

cycles. Indeed, a limitative factor of many applications is the cyclic behavior of the alloys [16]. A well-known phenomenon observed in NiTi is that their superelastic behavior evolves upon loading cycles. Basically, there is a drop in both forward and reverse transformation stresses and an increase in the residual strain which precludes for the stress–strain curves to be closed as an ideal superelastic cycle [17, 18]. Changes in the behavior can be of such magnitude that turns the NiTi element useful for the proposed application. That is why this evolution of the superelastic behavior is denominated "functional" fatigue in opposition to the "structural" fatigue, the failure of which involves the fracture of a superelastic member [19, 20]. Origin of functional fatigue is attributed to microstructural changes that occur in the material after a transformation. Among the mechanisms proposed for explaining the origin of the functional fatigue, the existence of retained martensite [21] and residual stresses due introduced dislocations [22] and selection of favored martensitic variants [23] are proposed by different authors. Probably, all of them are simultaneously active and coupled to each other as proposed in [24]. The microstructural evolution has been included in a constitutive model of NiTi alloys [25], making it possible to reproduce superelastic behavior at the first cycle. Pilch et al. [26] performed a systematic tuning of the parameters of an annealing treatment consisting in current micropulses with the aim of minimizing functional fatigue effects of NiTi wires.

A well-known phenomenon observed in NiTi wires is the localized character of the transformation in one or several fronts [27, 28]. Because of this particularity, the microstructural evolution upon cycling has place only in those portions of the material being swept by the fronts. If cycles of variable amplitudes are applied, an uneven evolution of the material will arise, affecting the resultant mechanical response of the material. In their experimental works on structural fatigue of NiTi wires, Jaureguizahar et al. [29, 30] take advantage of this uneven evolution. They restrict the affected zone to a central part of a wire specimen. In this way, it is possible to study structural fatigue in NiTi wires avoiding the interaction of the transformation fronts with the grips.

In this work, the effect of functional fatigue on the mechanical response of NiTi wires subjected to variable amplitude cycling is studied. A test program consisting in the application of four blocks of different amplitudes composed by a different number of cycles was applied to NiTi wire specimen, modifying the order by which the blocks were applied in each experiment. Results are rationalized by assuming the localized character of transformation in propagating fronts.

Material and Testing Details

The material used in the present work is a 0.5 -mm-diameter Ni-rich NiTi superelastic wire (50.8 at.% Ni) provided by SAES Getters in the straight annealing condition. Specimens with a length of 55 mm between grips were used for the mechanical tests which were carried out in an Instron 5567 electromechanical testing machine equipped with an Instron 3319 thermal chamber. The testing temperature was 35 °C in all cases. Measurement of force was performed with an Instron load cell with 5 kN maximum load and crosshead strain data were registered from the encoder system of the testing machine. Tests were performed under displacement control, using a constant crosshead velocity of 1 mm/min. Depending on the case, displacement or load limits were employed to define the cycle extremes. These values will be given in the description of each particular case. The mechanical response was described in terms of the stress–strain curves with the stress values calculated in terms of the initial cross section of the wire and the strain with the crosshead displacement and the initial free length of the wires between grips.

Test Programs and Results

With the aim of getting a reference frame of the superelastic behavior and functional fatigue characteristics of the NiTi wire employed, two pull–pull tests up to 160 complete cycles were firstly performed. After that, several cycling pull–pull tests using different imposed displacement limits were considered. A number of blocks of cycles with different constant amplitudes were applied following different sequences. The specific sequence followed in each case will be explained when describing the particular experiments in what follows.

Complete Cycle Tests—Effect of Cycle Accumulation on the Superelastic Behavior

As mentioned before, the first two tests consisted in 160 complete cycles. The limits for the first of these two experiments were set in 20 N on the low-displacement side and 4.4 mm on the high-displacement side, while for the second experiment they were set to 20 and 120 N, respectively. Figure 1a and b shows the stress–strain curves for the first (T1) and second (T2) tests, respectively. The main features associated with the functional fatigue of NiTi wires can be appreciated from these figures, i.e., a drop in both stress level plateaus and an accumulation of

Fig. 1 Results of complete cycle tests: **a** stress–strain curves of T1 test, with upper displacement limit. **b** Stress–strain curves of T2 test, with upper force limit. **c** Evolution of stress levels with the number of cycles. **d** Evolution of residual and maximum strains with cycle number
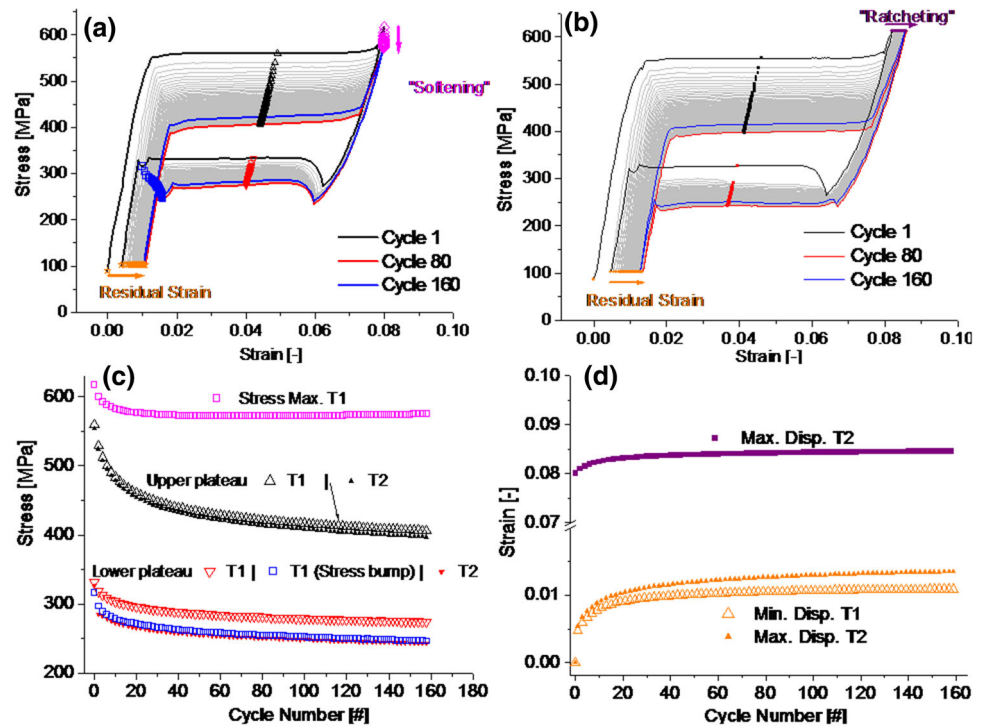
the residual displacement at the lower limit of each cycle. In the case of the T1 test, a progressive drop occurs in the maximum stress reached at the end of the cycle, while in the case of the T2 test a progressive drift of the maximum strain is observed (*ratcheting*). Both sets of stress–strain curves include a series of points representing the drop in the forward (black symbols) and reverse (red symbols) transformation stress plateau levels at approximately the mid-plateau position. A sort of bump can be observed at the end of the reverse transformation in cycles of T1. The explanation of this behavior is related to the localized character of the transformation. Depending upon the experimental conditions, the transformation can be completed by several moving fronts [29, 30]. The annihilation of one or two fronts produce an increase in the velocity of the remaining ones, from which results an overcooling and a drop in the stress due to the thermomechanical coupling. For a complete explanation of how thermal effects affect the mechanical response of superelastic NiTi, see for example [31, 32]. Residual strains are highlighted with orange symbols. Also the points indicating the maximum stresses reached in T1 (magenta symbols) and maximum strains in T2 (purple symbols) are included, highlighting the softening and ratcheting behavior, respectively. In the plot of Fig. 1c and d, it is possible to evaluate the evolution of the particular mentioned points as a function of the number of cycles. An asymptotic trend in all the cases is observed. Upper plateau stress exhibits the same evolution for T1 and T2. Both lower plateau stress levels evolve with

the same rate. From Fig. 1d, it can be observed that a higher accumulation of residual strains occurs in T2, thus indicating that the residual strains depend not only on the number of complete cycles but also on the maximum stress reached.

This first set of experiments therefore characterizes the general features associated with functional fatigue when the studied material is subjected to complete cycles. In the next section, these results are used to interpret the ones obtained when partial cycles of different amplitudes are applied to the same material.

Partial Cycle Test

Partial Cycle Test Programs

The following tests consisted in the application of four blocks of different numbers of cycle and amplitude. As shown in Fig. 2, each test consisted in the applications of blocks of 82, 42, 22, and 12 cycles of 1, 2, 3, and 4 mm of strain range corresponding to the total uniaxial strains of 1.8, 3.6, 5.5, and 7.3%, respectively. These blocks were applied with an increasing amplitude sequence, a decreasing amplitude sequence, and interleaved amplitudes as shown in Fig. 2b.

The previously described sequences were applied either starting from the fully austenite side, from the fully martensite side, or in the form of internal loops as illustrated in Fig. 3. They are referred to as full austenite partial

Fig. 2 Experimental program for partial cycle test: **a** block ranges and cycle counts. **b** Description of the amplitude ordering applied
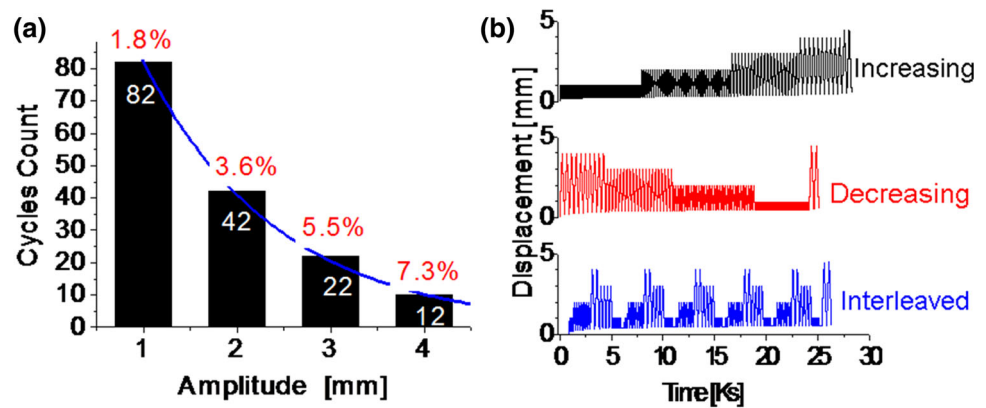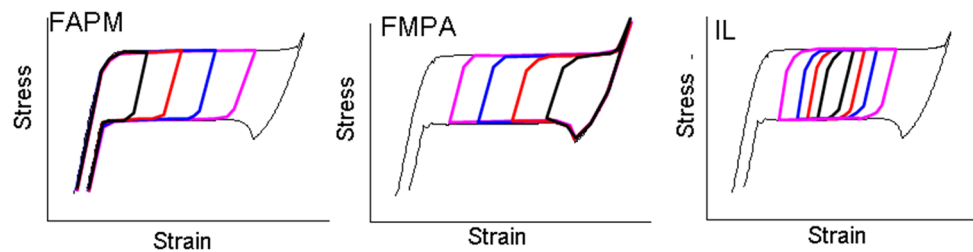

Fig. 3 Different kinds of partial loops performed during the partial cycle tests

martensite (FAPM, Fig. 3, left), full martensite partial austenite (FMPA, Fig. 3, center), and inner loops (IL, Fig. 3, right). FAPM tests were performed by setting up a lower force limit of 20 N on the lower strain side, while FMPA tests were performed using an upper force limit of 120 N on the high-displacement side.

In summary, the extensive experimental program carried out in the present work combined in principle the three types of partial cycles with three sorts of ordering sequences. One exception was the combination of inner loops with interleaved ordering which was not included in the test program. Thus, this results in a total of eight variable amplitude types of experiments. After being subjected to the whole sequence of variable amplitude blocks in each test, the final mechanical response of the wire was recorded by performing two successive complete cycles at the end of each test. In that way, the overall effect of the different sequences on the resulting pseudoelastic behavior could be compared. The number of cycles selected for each block was originally set to 80, 40, 20, and 10 cycles, i.e., following a geometric progression. Two more cycles were added to each block in such a way that, including the two complete final cycles, a whole test totalizes 160 cycles, as for T1 and T2.

FAPM Tests with Increasing and Decreasing Ordering Sequences

The first test of this type corresponds to a FAPM with increasing amplitudes. The resulting stress–strain curves are presented in Fig. 4a–d, starting with the cycles of the first block which has the lowest strain range. In gray lines, the complete stress–strain history is included until the end of each block, and the first and last cycles are highlighted in colored thin and thick lines, respectively. Functional fatigue seems to affect the response of the wire in the same way that it does in complete cycles, i.e., there is a drop in the plateau stress and residual strain accumulation which are indicated using black points in Fig. 4a. However, it is observed that when strain approximates the first upper limit the stress rises to a level similar to the one corresponding to the first cycle. This can be clearly observed in the last cycle of the block depicted in thick black line in Fig. 4a. This stress rising indicates that the involved transformation fronts are arriving to the zone of virgin material which was still not subjected to the transformation. When the second block with a higher range of 2 mm starts, a new portion of the material is involved in the transformation. This is reflected in the shape of the first cycle of the second block in Fig. 4b where an upper plateau with two distinct stress levels is observed. Further, these zones associated with two volumes with different cycle numbers evolve independently. At the end of the block, the cycle in thick red line presents the upper plateau with two levels, one reflecting the stress drop corresponding to $82 + 42 = 124$ and the other to 42 cycles. A similar analysis can be performed with the third block. Cycles in blue in Fig. 4c presents three upper level plateaus, indicating that there are three zones of the material with different loading histories. Finally, the fourth block shown in Fig. 4d expands further the material involved in the transformation. Both the first and last cycles of the block in magenta show four different

Author's personal copy

Shap. Mem. Superelasticity

Fig. 4 a–d Stress–strain curves associated with each amplitude block obtained from the FAPM increasing amplitude tests. The first and last cycles of each block are highlighted with colored thick lines. Black, red, blue, and magenta colors correspond to blocks 1, 2, 3, and 4, respectively (Color figure online)
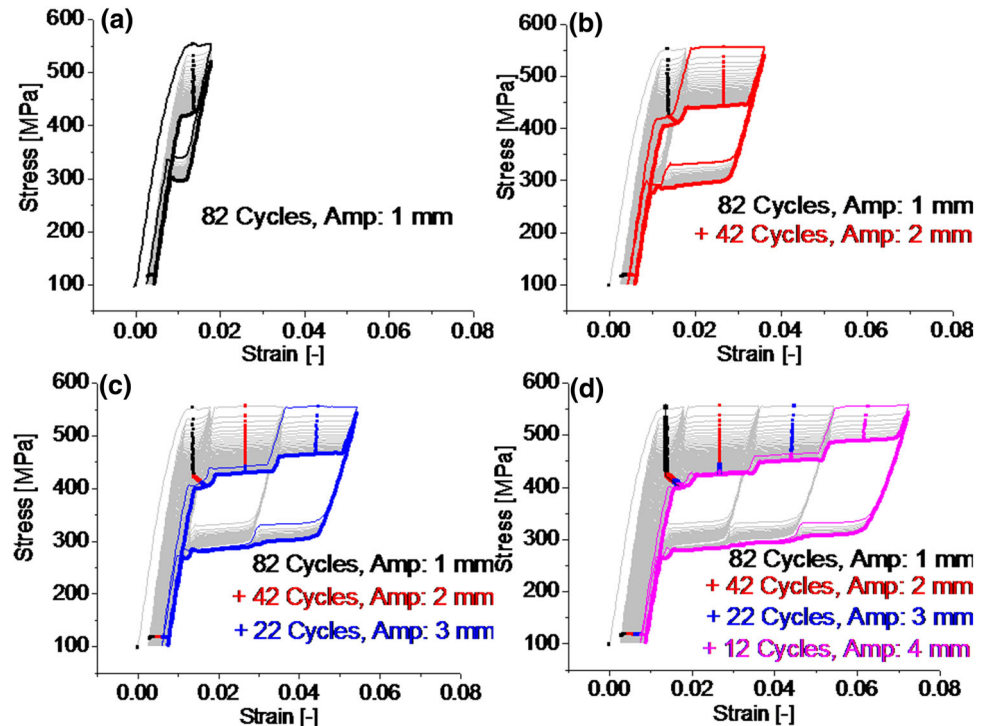
stress levels in the upper plateau. The points in black, red, blue, and magenta included in each of the figures indicate the track of the force drop and residual accumulation registered during the first, second, third, and fourth blocks. Black, red, blue, and magenta colors correspond to blocks 1, 2, 3, and 4, respectively, and the same color representation will be also used for the rest of the tests unless otherwise specified.

In the next test, FAPM blocks with a decreasing amplitude ordering were performed. Results are shown in Fig. 5, following the same scheme as in the previous test. The first and last cycles of each block are highlighted with thin and thick colored lines, respectively. In this case, the first block, shown in Fig. 5a, is the one with the highest amplitude. Cycles exhibit the general characteristics of functional fatigue. When the second block (Fig. 5b) begins, the volume of material involved in the transformation is smaller. If it is assumed that the portions of material most favorable to be transformed from austenite to martensite are those exhibiting the lowest transformation stress, it can be affirmed that the volume of the material involved in transformation during block 2 is included in the volume corresponding to block 1. Therefore, there is only one stress level for the upper plateau. Similarly, the cycles of the third block shown in Fig. 5c involve now an even smaller volume of the previous cycled material in the transformation. In the fourth block, corresponding to cycles of 1 mm of range, it is observed how the current displacement range of the cycles has decreased due to

the residual strain accumulated during the previous stages. As in Fig. 4, the colored points in each figure represent the stress drop and the residual strain accumulated in each block.

As it was mentioned before, at the end of each test two complete cycles were performed with the aim of registering the resultant state of the wire. In Fig. 6a, the final complete cycles after the increasing, decreasing, and interleaved ordering tests are compared. For comparison, the cycle number 160 corresponding to the type T1 complete cycles is included as a reference cycle. The stress–strain curves of the three complete cycles obtained at the end of the variable amplitude cycling tests present an additional level of the upper plateau associated with the material which transformed just in the two final complete cycles. The mechanical responses of the three wires were similar. In these cases, it is possible to associate a part of the stress–strain curve with a portion of the material volume for a certain number of cycles. An important conclusion that can be drawn from these results is that the behavior of the wire depends on the previously applied variable amplitude cycles but not on the order in which they were applied.

In Fig. 6b, the evolution of residual strains with cycle number for the three different sequences described are presented together with the residual strains corresponding to T1 test as a reference. Accumulated residual strains for the three sequences remain lower than the ones of T1. Results corresponding to increasing amplitude sequence are illustrative for the understanding of the local

Springer

Fig. 5 **a–d** Stress–strain curves associated with each amplitude block obtained from the FAPM decreasing amplitude tests
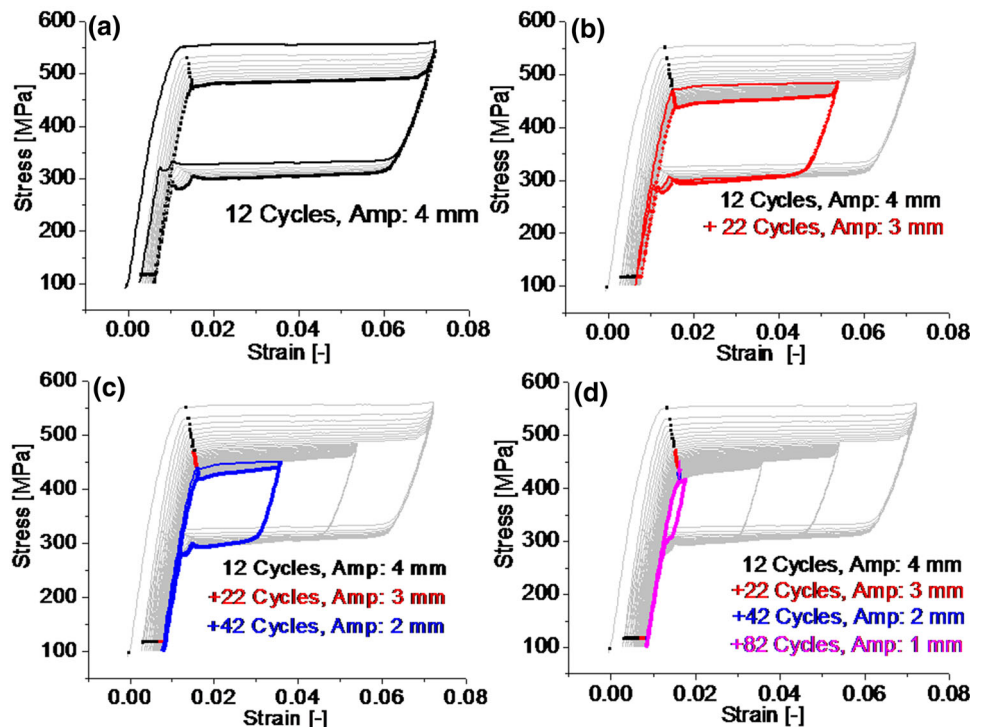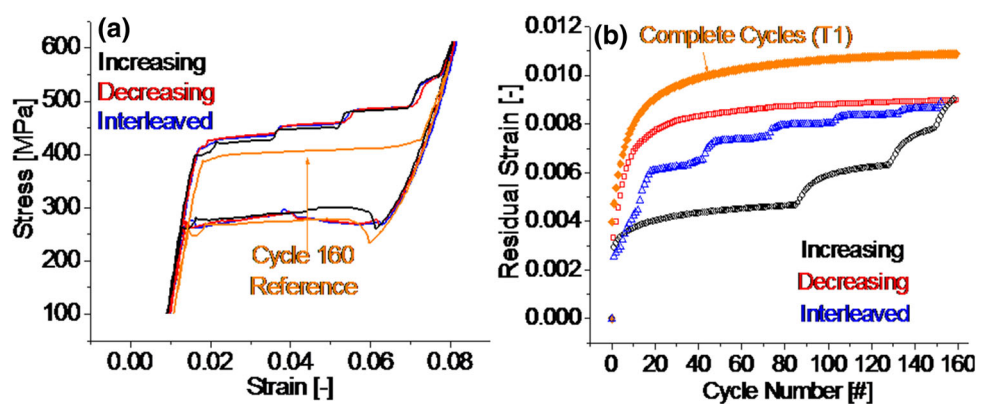

Fig. 6 Summary of FAPM test results: **a** comparison of the final complete cycles obtained after each partial amplitude test and the last complete cycle of test T1. **b** Evolution of residual strains with the number of cycles

contribution to the total residual strain. The residual strain rate seems to follow an asymptotic trend with the steady value step augmenting each time the amplitude is increased. Each time a new portion of material is involved in the transformation, it starts contributing to the total residual strain as a "virgin" material. In the curve corresponding to the decreasing amplitude sequence, changes in the asymptotic trend associated with the beginning of a new block are not clearly appreciated. In this case, the saturation value decreases in each new block since the transforming volume of the associated material lies enclosed inside the previously cycled one.

A conclusion that is worth to point out is that the accumulated residual strains obtained after applying the same type of variable amplitude cycles are not influenced by the order in which they are applied. This behavior

suggests that a sort of linear damage like the Miner's rule used in structural fatigue can be considered here to evaluate the effect of partial cycling on the accumulate residual strain. The total residual strain would then result from the contribution of the material domains with different cycling histories. While each cycle involves a determined active material volume, the ordering sequence should not affect the total accumulated residual strain.

FMPA Tests with Increasing and Decreasing Ordering Sequences

The next set of variable amplitude cycles corresponds to those starting from a fully martensite state. The increasing, decreasing, and interleaved ordering sequences were repeated for this kind of cycles. Figure 7a–d summarizes

Author's personal copy

Shap. Mem. Superelasticity

the stress–strain curves from the increasing amplitude ordering test. The upper limit for these tests was set to 120 N. During the first block consisting in 82 cycles with a displacement range of 1 mm, almost no evidence of reverse stress-induced transformation can be observed (Fig. 7a), i.e., the wire remained in martensite condition. The second block, in Fig. 7b, involves clearly a volume of the material that undergoes first a reverse transformation to austenite and then a partial austenite to a fully martensite state cycling. The characteristic drop in the transformation stress plateaus associated with functional fatigue is again observed. It occurs during the third block, depicted in Fig. 7c, when a clear extension of the transformed volume occurs. As in the rest of the figures, the last cycle is highlighted using colored line. In this case, the first cycle of the block has been included in blue empty circles to facilitate the analysis. The first cycle of block 3 starts upon unloading from the upper limit. This follows a path similar to the one of the last cycle of block 2 (red line curve in Fig. 7b). Then, the transformation volume is extended by adding a portion of the material which has been so far in martensite. It is observed that for continuing with the reverse transformation there are a sharp stress drop and then a rise in the force until a stress level even higher than the one for the first part of the reverse transformation is reached. Thus, a stress barrier associated with the sharp stress drop has to be overcome for the reverse transformation to advance in the part of the material that so far has

never reverse transformed to austenite. On further loading, the upper plateau exhibits two stress levels. The one with the lower force is associated with the portion of material that was already cycled during block 1, while the second is associated with the new active volume. Unlike what happens with FAPM cycles, in this case it is not possible to associate a part of the stress–strain curve with a partial transforming volume along the whole test. This relationship between transformation volumes and segments of the stress–strain curves is described in more detail in "IL Tests with Increasing and Decreasing Ordering Sequences." For the fourth block, included in Fig. 7d, there is another extension of the material domain involved in the transformation. The last cycle of this block represented in magenta allows observing that the end of the reverse transformation is reached with an important residual strain accumulated during the test.

The test of FMPA with decreasing amplitude is now described. The stress–strain curves after each block are included in Fig. 8. This test presents some similarities with the FAPM decreasing amplitude, as shown in Fig. 5. For both tests, a new block involves a smaller transforming volume which is enclosed in the previously cycled material volume. In this case, during the first block of 4 mm of amplitude in Fig. 8a, the cycles do not include the end of the reverse transformation as observed for the same amplitude in the previous test (Fig. 7d). This is explained because the residual strains are not high enough at this

Fig. 7 a–d Stress–strain curves associated with each amplitude block obtained from the FMPA increasing amplitude tests
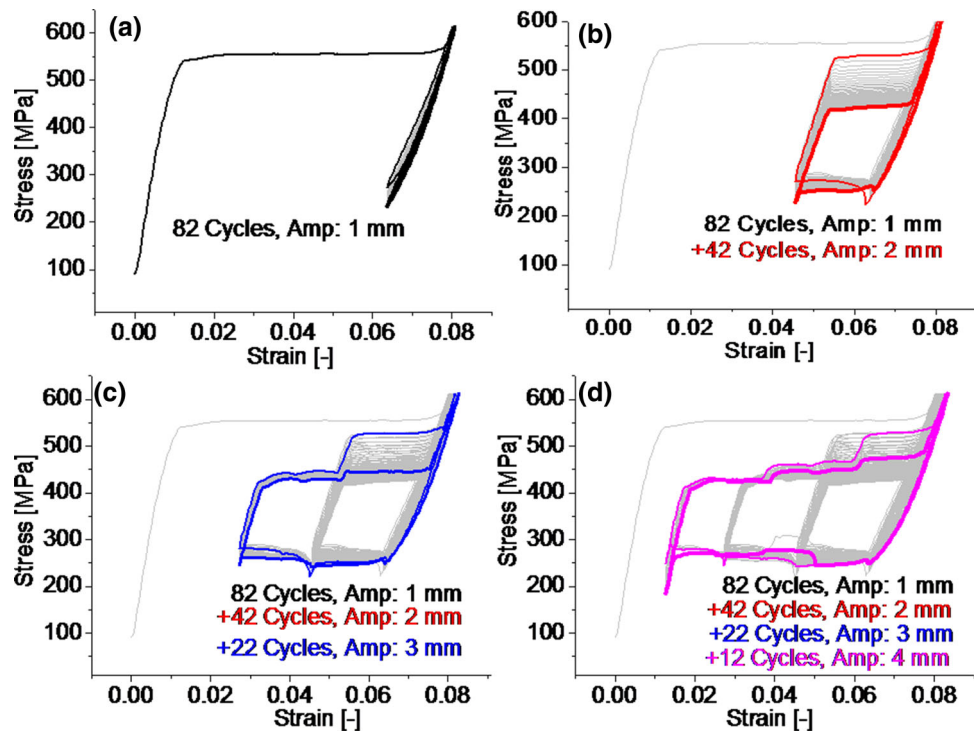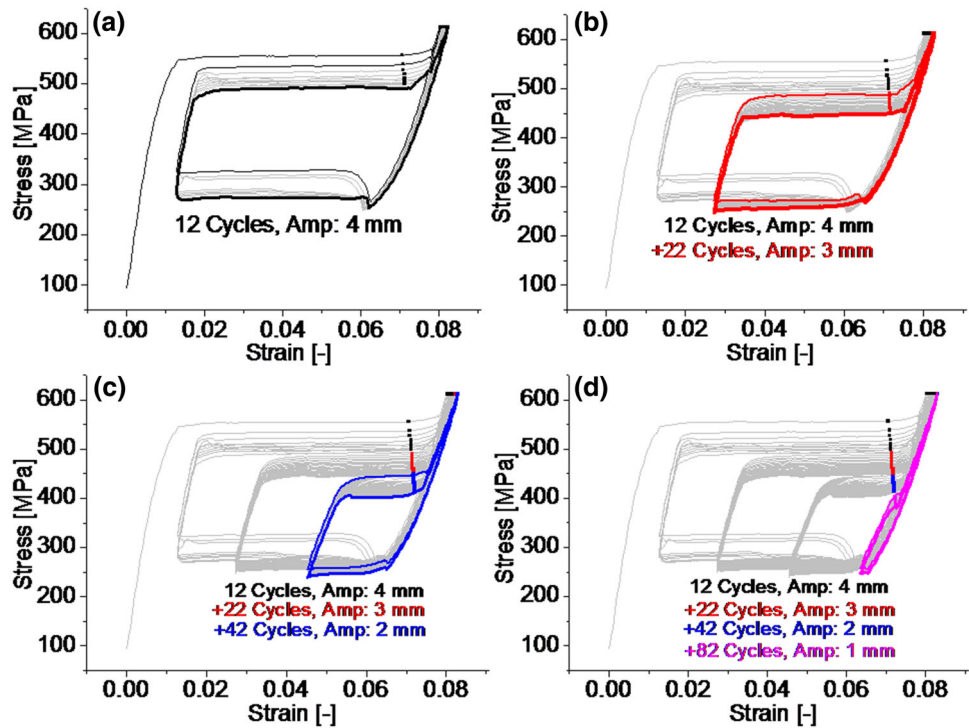
Springer

Fig. 8 a–d Stress–strain curves associated with each amplitude block obtained from the FMPA decreasing amplitude tests

point of the experiment and the cycle remains as a partial one.

In Fig. 9a, the final complete cycles performed at the end of the FMPA increasing, decreasing, and interleaved ordering tests are compared. There exist reasonable similarities for the same conclusions that in the case of FAPM cycles to be drawn, i.e., the order in which cycles of variable amplitudes are applied to the superelastic NiTi does not affect the final state. For this kind of cycles, it is not possible to track the residual strain accumulated along the tests. Instead, the drift in the maximum strain was used as a measure of the progressive damage shown in Fig. 9b. Results from the three ordering sequence tests show a drift lower than the one registered for the complete cycle test T2. In this case, while for the increasing and interleaved ordering sequences the accumulated drift seems to

approach the same value, for the decreasing order a lower level is reached.

IL Tests with Increasing and Decreasing Ordering Sequences

The last set of experiments corresponds to the inner loops (IL). The amplitudes of the cycles were measured around a middle position fixed at a displacement (strain) of 2 mm (0.036), and therefore the lower and upper limits were 1.5 mm (0.027) and 2.5 mm (0.045) for block 1, 1 mm (0.018) and 3 mm (0.055) for block 2, 0.5 mm (0.009) and 3.5 mm (0.064) for block 3, and 0 mm (0) and 4 mm (0.073) for block 4. Additionally, a lower force limit of 20 N was set up. Since this load level is imposed with the aim of avoiding for the wire to get loose once residual

Fig. 9 Summary of FMPA test results: **a** comparison of the final complete cycles obtained after each partial amplitude test and the last complete cycle of test T2. **b** Drift of the maximum strain at the end of each cycle as a function of the number of cycles
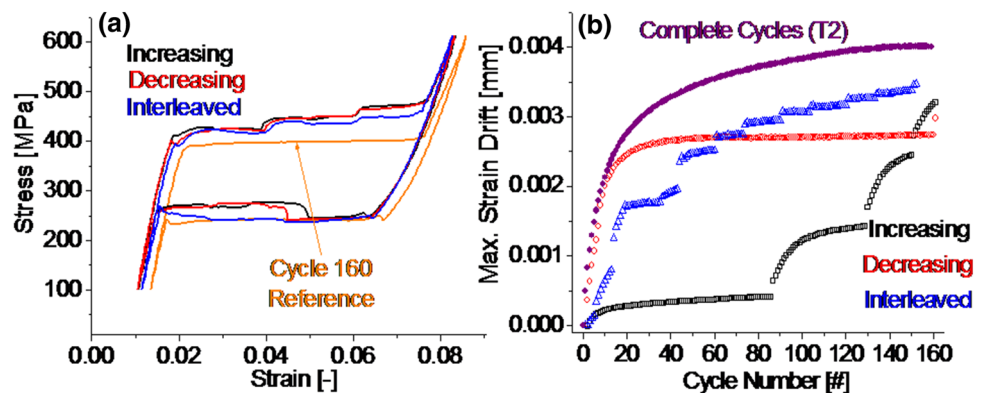
strain start to accumulate, it is prioritized over the displacement level. In the case that this lower force limit is reached before the displacement level, the unloading is interrupted and a new cycle starts.

Only increasing and decreasing ordering sequence tests were performed for this kind of cycles. Figure 10a–d shows the stress–strain curves of the increasing ordering sequence with the first and last cycles highlighted with colored lines. Cycles of the first block between the displacement limits of 1.5 and 2.5 mm show the drop in the transformation stresses. The last cycle, in thick black line, shows a stress rising when the upper limit is approached and a smaller stress drop when the lower limit is approached. For the sake of clarity, what occurs with the material response when block 2 starts is explained separately in Fig. 11. This figure represents the last cycle of block 1 with black line and the first cycle of block 2 with red line. To the right of the graph, there are different portions of the material schematized in different colors at the end of block 1 and after the first cycle of block 2. Volume 1 corresponds to the material which stayed in the austenite phase, volume 2 to the one which remained in the martensite phase, and volume 3 is the material domain involved in the transformation during block 1. Then, during block 2 the transformation domain adds volume 4 from volume 1 and volume 5 from volume 2. The fact that the new material involved in the transformation comes from different portions is a distinctive characteristic of this kind of cycles. When block 2 starts, following the path A in the graph, the stress reaches

the level of a first cycle upper plateau. This is because volume 4 is being transformed for the first time to martensite. Then, reverse transformation starts along path B and on volume 4 which has the highest lower plateau stress since it is its first reverse transformation. Next, path C copies the segment of the last block 1 cycle, corresponding then to volume 3. Then, volume 5 goes from martensite to austenite for the first time through path D. For this reverse transformation to occur, the barrier caused by the stress drop at the beginning of path D is needed to be overcome. This stress barrier would be associated with the necessity for a new austenite domain to be nucleated in a martensite volume. Then, the force reaches a level higher than the one along path C. This situation was already presented in Fig. 7c, for the FMPA increasing amplitude test. Following the strain reversal, the cycle continues with loading along path E. The first part of the forward transformation plateau exhibits the lowest stress level, being associated with volume 3, i.e., the material already subjected to cycling. Finally, path F indicates a middle plateau stress level. This corresponds to the forward transformation of volume 5, whose material had already completed one cycle before.

The final test was the program of IL cycles with a decreasing ordering sequence. Figure 12 shows the stress–strain curves associated with each block, as it is done for the rest of the tests. As occurred in the other tests with decreasing sequences, each time a new block starts, the volume involved in the transformation is smaller and

Fig. 10 a–d Stress–strain curves associated with each amplitude block obtained from the IL increasing amplitude tests
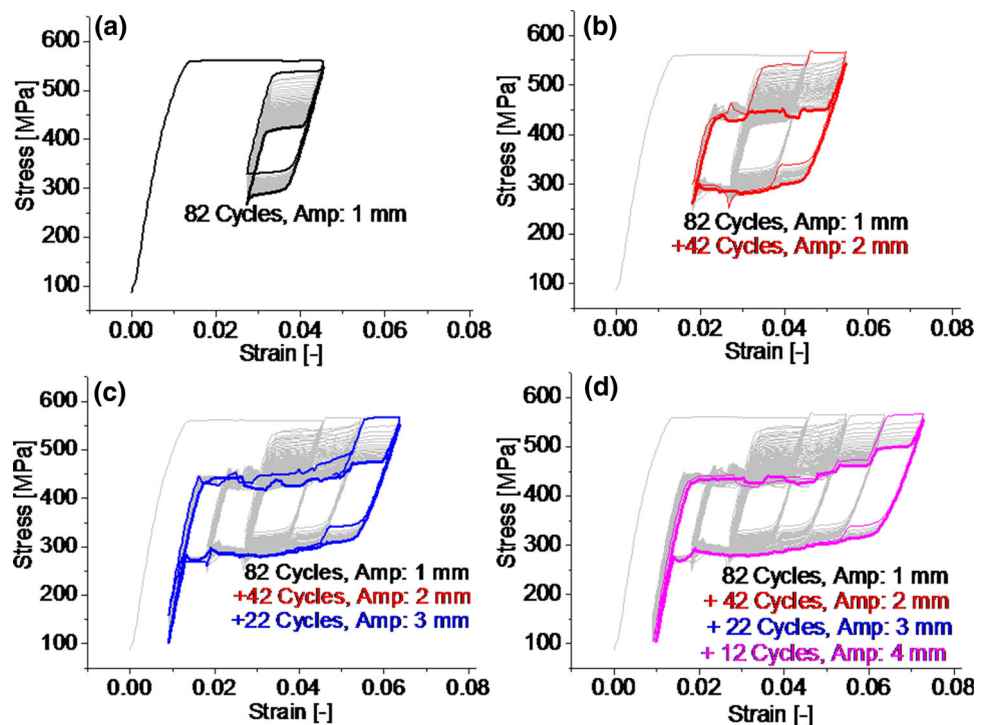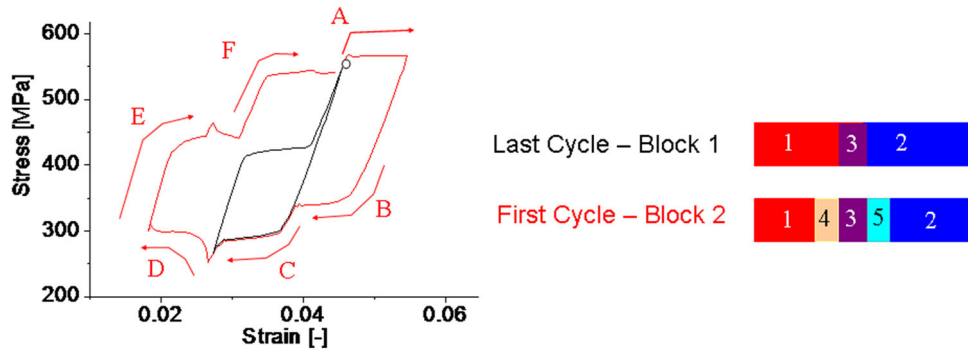
Fig. 11 Left: the last cycle of block 1 in black line and the first cycle of block 2 in red line. Right: identification of the different material portions or domains according to their loading history. Volume 1: portion in austenite during block 1. Volume 2: portion in martensite during block 1. Volume 3: portion involved in transformation during block 1. Volume 4: portion involved in transformation during block 2 formerly belonging to volume 1. Volume 5: portion involved in transformation during block 2 formerly belonging to volume 2 (Color figure online)

Fig. 12 a–d Strain–stress curves associated with each amplitude block obtained from the IL decreasing amplitude tests
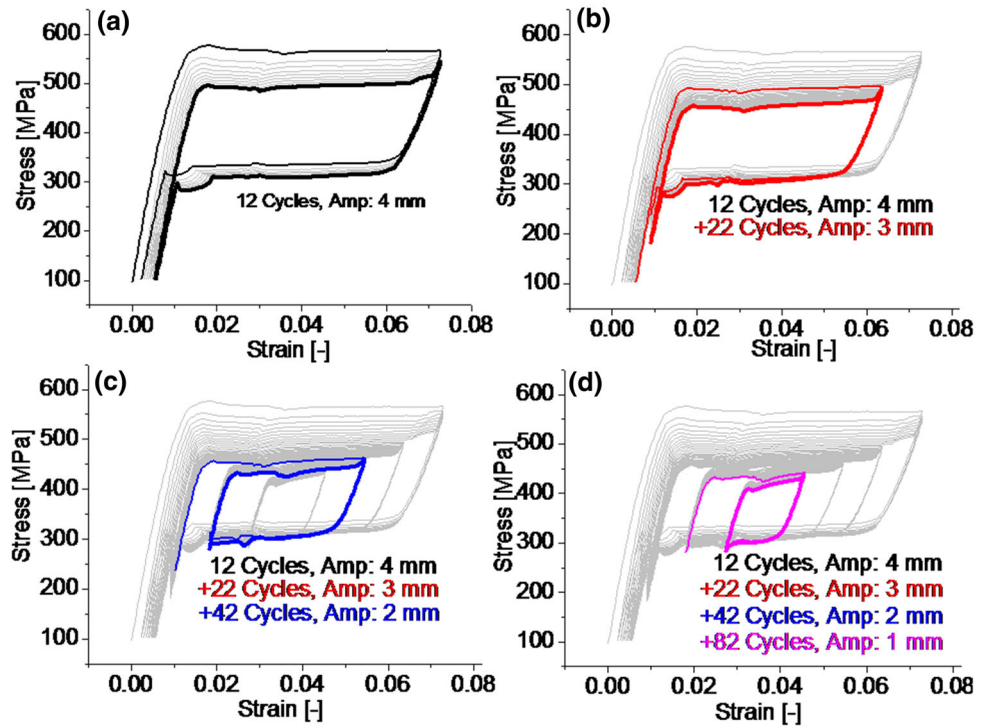
included in the previous transforming volume. Stress–strain curves exhibit the stress drops associated with functional fatigue. The amplitude in block 1 is high enough for the cycle to complete the reverse transformation (Fig. 12a). Accumulation of residual strain after the first cycle produces a shifting in the initial point of further cycles, which results in a range lower than the programmed 4 mm. It can be observed that reverse transformation is completed also by cycles of block 2 in Fig. 12b.

In Fig. 13, complete cycles performed at the end of both IL increasing and decreasing ordering sequence tests are compared. Although the same trend can be observed for the upper plateau in both cycles, with an increasing stress
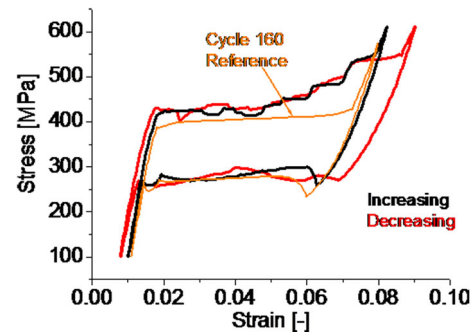

Fig. 13 Comparison between the last complete cycles after IL increasing and decreasing amplitude tests

toward their end, they exhibit an irregular shape and it is not possible to associate the mechanical response with the applied loading history as it was done in Figs. 9a and 6a.

Final Remarks and Conclusions

Comparison of final states from FAPM or FMPA cycles with different ordering sequences suggests that whatever the order in which cycles of different amplitudes are applied to a virgin NiTi wire, the resultant mechanical response of the material is approximately the same.

The residual strains for the FMPA cycles evolve differently for the different ordering sequences, but for the three tests a similar final value is obtained. This allows for establishing a linear damage rule, for which the residual strains result from the proportional contribution of the different cycling volumes. This rule does not completely apply to the FAPM cycles, for which the decreasing ordering sequence resulted in lower values of maximum residual drift.

These conclusions based on the experimental results support the adopted interpretation criterion: the localized character of the transformation allows assuming that partial cycles involve transformation in partial volumes, the sizes of which are related to the corresponding amplitudes. Each volume presents functional fatigue resulting from its local cycling history, i.e., with the number of times a localized transformation front sweeps the region.

The formation of the stress barrier at the positions on the reverse transformation where the fronts revert their movement during a constant residual amplitude block represents an additional factor to be considered if a precise model describing the general evolution of the superelastic response needs to be formulated. Further research would also be needed to clarify the microstructural reasons behind this phenomenon.

References

1. Otsuka K, Wayman C (1998) Shape memory materials. Cambridge University Press, Cambridge
2. Chan Y, Cheng S (2016) Angioplasty and stenting of distal anastomotic stenosis of femoropopliteal bypass graft using helical interwoven nitinol stents. Int J Angiol 25(05):e25–e58
3. Setiyorini Y, Pintowantoro S (2013) Biocompatibility improvement of NiTi orthodontic wire from various coatings. Adv Mater Res Switz 789(11):225–231
4. Liang T, Chang L, Wei-Xuan L, Yao-Jiang Z (2017) Superelastic behavior analysis of shape memory alloy vascular stent. Key Eng Mater 725(2):405–409
5. Wang G, Shen Y, Cao Y, Yu Q, Guidoin R (2007) Biocompatibility study of plasma-coated nitinol (NiTi alloy) stents. IET Nanobiotechnol 1(6):102–106
6. Takashi M, Toshiaki M, Yoshiyuki W, Seiya K, Youichi H, Masayoshi E (2002) An active guide wire with shape memory alloy bending actuator fabricated by room temperature process. Sens Actuators A Phys 97:632–637
7. Soul H, Yawny A (2002) Self-centering and damping capabilities of a tension-compression device equipped with superelastic NiTi wires. Smart Mater Struct 24:075005
8. Ozbulut O, Hurlebaus S, Desroches R (2011) Seismic response control using shape memory alloys: a review. J Intell Mater Syst Struct 22:1531–1549
9. Engeberg E, Dilibal S, Vatani M, Choi J, Lavery J (2015) Anthropomorphic finger antagonistically actuated by SMA plates. Bioinspir Biomim 10:15
10. Elahinia M (2016) Shape memory alloy actuators: design, fabrication, and experimental evaluation. Wiley, Hoboken
11. Buban D, Frantziskonis G (2013) Shape memory alloy fracture as a deployment actuator. Smart Mater Struct 22:10
12. Lee M, Jo J, Won-Jun Tak W, Kim Byungkyu (2011) Shape memory alloy (SMA) based non-explosive separation actuator (NEA) with a redundant function. Int J Precis Eng Manuf 12(3):569–572
13. Xiaofeng Lu, Li Gang, Liu Luwei, Zhu Xiaolei, Shan-Tung Tu (2017) Effect of aging treatment on the compressibility and recovery of NiTi shape memory alloys as static seals. J Mater Eng Perform 26(7):3025–3033
14. Schmidt M, Schütze A, Seelecke S (2016) Elastocaloric cooling processes: the influence of material strain and strain rate on efficiency and temperature span. APL Mater 4:064107
15. Garrett J, Pataky G, Ertekin E, Sehitoglu H (2015) Elastocaloric cooling potential of NiTi, Ni2, FeGa, and CoNiAl. Acta Mater 96:420–427
16. Mahtabi M, Shamsaei N, Mitchell M (2015) Fatigue of nitinol: the state-of-the-art and ongoing challenges. J Mech Behav Biomed 50:228–254
17. Yawny A, Sade M, Eggeler G (2005) Pseudoelastic cycling of ultra-fine-grained NiTi shape-memory wires. Z Metallkd 96(6):608–618
18. Schlun M, Zipse A, Dreher G, Rebelo N (2010) Effects of cyclic loading on the uniaxial behavior of nitinol. J Mater Eng Perform 20(4–5):684–687
19. Eggeler G, Hornbogen E, Yawny A, Heckmann A, Wagner M (2004) Structural and functional fatigue of NiTi shape memory alloys. Mater Sci Eng A 378:24–33
20. Olbricht J, Yawny A, Condo A, Lovey F, Eggeler G (2008) The influence of temperature on the evolution of functional properties during pseudoelastic cycling of ultra fine grained NiTi. Mater Sci Eng A 481–482:142–145
21. Isalgue A, Soul H, Yawny A, Auguet C (2015) Functional fatigue recovery of superelastic cycled NiTi wires based on near 100 °C aging treatments. In: MATEC Web of Conferences 03019
22. Tan G, Liu Y, Sittner M, Saunders M (2004) Lüders-like deformation associated with stress-induced martensitic transformation in NiTi. Script Mater 50(2):193–198
23. Miyazaki S, Imai T, Igo Y, Otsuka K (1986) Effect of cyclic deformation on the pseudoelasticity characteristics of Ti–Ni alloys. Metall Trans A 17A(1):115–120
24. Manchiraju S, Anderson P (2010) Transformation-induced plasticity during pseudoelastic deformation in Ni–Ti microcrystals. Int J Plast 26:1508–1526
25. Petrini L, Bertini A, Berti F, Pennati G, Migliavacca F (2017) The role of inelastic deformations in the mechanical response of endovascular shape memory alloy devices. Proc Inst Mech Eng H 231(5):391–404

26. Dellville R, Malard B, Pilch J, Sittner P, Schryvers D (2010) Microstructure changes during non-conventional heat treatment of thin Ni–Ti wires by pulsed electric current studied by transmission electron microscopy. Acta Mater 58:4503–4515

27. Shaw J, Kyriakides S (1995) Thermomechanical aspects of NiTi. J Mech Phys Solids 43:1243–1281

28. Schlosser P, Favier D, Louche H, Orgéas L, Liu Y (2009) From the thermal and kinematical full-field measurements to the analysis of deformation mechanisms of NiTi SMAs (ESOMAT 2009, September 2009 Czes Republic). In: Proceedings of the 2009 ESOMAT, EDP Science

29. Jaureguizahar S, Soul H, Chapetti M, Yawny A (2015) Characterization of fatigue life of ultrafine grained NiTi superelastic wires under uniaxial loading. Proc Mater Sci 9:326–334

30. Jaureguizahar S, Chapetti M, Yawny A (2016) Fatigue of NiTi shape memory wires. Proc Struct Integr 2:1427–1434

31. Soul H, Yawny A (2013) Thermomechanical model for evaluation of the superelastic response of NiTi shape memory alloys under dynamic conditions. Smart Mater Struct 22:035017

32. He Y, Sun Q (2010) Rate-dependent domain spacing in a stretched NiTi strip. Int J Solid Struct 47:2775–2783